Modeling of a Terfenol-D ultrasonic transducer

Julie C. Slaughter*[a], Marcelo J. Dapino[b], Ralph C. Smith[c], Alison B. Flatau[b]

[a]ETREMA Products, Inc., Ames, IA 50010

[b]AEEM Department, Iowa State University, Ames, IA 50011

[c]Center for Research in Scientific Computation, North Carolina State University, Raleigh, NC 27695

ABSTRACT

A large variety of applications exist which take advantage of the high dynamic strain and high energy coupling factor exhibited by "giant" magnetostrictive materials. One such material is the rare earth-iron compound Terfenol-D ($Tb_{0.3}Dy_{0.7}Fe_{1.95}$), which is being increasingly used in industrial, biomedical and defense applications. In order to fully realize the performance of this material, it is necessary to accurately model magnetostrictive transducer behavior from DC through the low ultrasonic regimes where the material is used. This paper has been motivated by the need for physically-based performance models of magnetostrictive materials as used in transducers. To this end, a recent magnetoelastic model for magnetostrictive transducers is employed to characterize the magnetization and strain behavior of Terfenol-D at frequencies from 1 Hz to 30 kHz. Model simulations were compared to experimental measurements at various drive levels and frequencies of operation, both under magnetically unbiased and biased conditions. The model provides an accurate characterization of the magnetization and strain for all operating conditions studied. However, further progress in strain simulations may be achieved through improvements in minor loop closure techniques and additional parameter identification.

Keywords: Terfenol-D, transducer model, ultrasonic, magnetostrictive, giant magnetostrictive material.

1. INTRODUCTION

Ultrasonic transducers are in widespread use for industrial processes such as industrial cleaning, chemical processing, and ultrasonic welding. The earliest materials used to make ultrasonic transducers were magnetostrictive materials such as nickel and piezoelectric materials such as quartz crystals.[1,2] Today, nickel is still widely used in industrial cleaning and chemical batch processing applications that utilize ultrasonic frequencies in the tens of kHz.[3] Quartz crystals have been widely replaced by piezoelectric materials with higher strain capabilities such as PZT's. Piezoelectric materials are typically used in very high frequency ultrasonics, MHz, for nondestructive evaluation applications. These materials are also used in high power devices for industrial processing.

The current state of ultrasonic technologies has reached a plateau. In order to realize a significant increase in industrial processing capabilities, ultrasonic transducers need to employ more capable driver materials. One material that has the potential to make a significant impact on the ultrasonic industry is the highly magnetostrictive material Terfenol-D. For instance, a predicted 25 kW ultrasonic transducer is under development with funding from the National Institute of Standards and Technology (NIST) Advanced Technology Program.[4] Anticipated applications for this technology include devulcanization of rubber and continuous chemical processing. However, in order to fully realize the potential of Terfenol-D at ultrasonic frequencies, it is necessary to develop predictive models capable of characterizing transducer behavior in design and control applications.

In order to take full advantage of the material's capabilities, it is necessary to develop a model capable of predicting behavior over a broad range of operating regimes. Highly magnetostrictive materials such as Terfenol-D exhibit nonlinear behavior. In addition, these materials exhibit magnetomechanical coupling. That is, the mechanical state of the material affects the magnetic state and vice versa. This phenomenon makes sensing with Terfenol-D possible. However, it also complicates the modeling in applications where large changes in the stress state of the material occur. A model incorporating both the nonlinear and magnetomechanical behaviors of Terfenol-D is a necessary step towards improving design capabilities.

* Correspondence: E-mail: julie.slaughter@etrema-usa.com; Telephone: 515 296-8030; Fax: 515 296-6620

In *Smart Structures and Materials 2000: Smart Structures and Integrated Systems*, Norman M. Wereley, Editor, Proceedings of SPIE Vol. 3985 (2000) • 0277-786X/00/$15.00

Models based on the linear constitutive piezomagnetic equations[5] have been used to simulate transducer behavior over a limited range of operation. Linear models can be used when a transducer is being utilized in a magnetically biased state with small magnetic drive fields and relatively constant stresses, i.e., under light loads. However, linear models are highly insufficient for high drive fields or high mechanical loading. While the scope of linear constitutive models has been extended by including specific nonlinear effects,[6,7] the usefulness of these models is limited by the availability of characterization data over a large range of operating conditions. This need for characterization data severely constrains the scalability of the results and complicates the implementation when operating conditions vary.

A variety of models have been developed based on phenomenological behavior. Among these are Preisach models specifically tailored to giant magnetostrictive materials.[8,9,10] Another category of models is based on a combination of physical laws and phenomenological behavior.[11,12] Many of these models are limited because they are purely material models and do not incorporate dynamical effects arising from transducer operation. A model which describes Terfenol-D magnetization behavior has been proposed by Calkins.[13] While some aspects of the model are phenomenological in nature, the small number of model parameters (five) and the traceability of these parameters to measurable quantities provides useful insight on the physical behavior of magnetostrictive materials. This model was later extended to incorporate transducer dynamical effects as well as the bidirectional energy coupling between the magnetic and elastic states.[14] In the work presented here, this transducer model is adapted to the configuration of a Terfenol-D ultrasonic transducer and extended to include eddy current effects.

The transducer model presented here is a powerful tool for both researchers and design engineers. In principle, a single set of parameters, once identified, can fully describe the behavior of Terfenol-D over a wide range of operating conditions. The model is fully coupled, which makes it possible to extend the model usage to sensor designs.[15] The nature of the model allows for transducer characterization in a variety of configurations and loading situations. Experimental results are presented which demonstrate the accuracy of the model over a broad range of operating conditions.

2. MODELING APPROACH

The model presented here builds upon a magnetomechanical transducer model proposed previously.[14] Eddy current effects are incorporated into the magnetization model to extend its usage to higher frequencies. In addition the model is modified to represent the configuration of an ultrasonic transducer.

Neglecting temperature effects, the magnetization is dependent on both the applied magnetic field and the stress state of the material. A general equation for the time rate of change of magnetization is given by Equation 1, which depends on both the differential susceptibility $\partial M/\partial H$ and the change in magnetization due to stress $\partial M/\partial \sigma$,

$$\frac{dM}{dt} = \frac{\partial M}{\partial H}\frac{dH}{dt} + \frac{\partial M}{\partial \sigma}\frac{d\sigma}{dt}, \tag{1}$$

where H is the applied magnetic field and σ is the stress in the Terfenol-D. A frequency dependent model of the differential susceptibility will be presented along with a law of approach to represent the magnetomechanical effects. A dynamic transducer model will be used to provide feedback of externally applied stresses to the magnetization.

2.1 Differential susceptibility

In order to use the model at ultrasonic frequencies, it is necessary that the differential susceptibilitiy $\partial M/\partial H$ includes frequency-dependent effects such as eddy currents. The model used for differential susceptibility, Equation 2, has been proposed in [17]. This model adds eddy current effects to a magnetic hysteresis model previously described by Jiles and Atherton.[16]

The first term in Equation 2 represents classical eddy current losses, anomalous losses are represented by the second term, and the remaining terms constitute the Jiles and Atherton magnetization model,[16,17]

$$\left(\frac{\mu_0 d^2}{2\rho\beta}\frac{dH}{dt}\right)\left(\frac{dM}{dH}\right)^2+\left(\frac{GdwH_o}{\rho}\right)^{1/2}\left(\frac{dH}{dt}\right)^{1/2}\left(\frac{dM}{dH}\right)^{3/2}$$
$$+\left(k\delta-\alpha\left(M_{an}-M+k\delta c\frac{dM_{an}}{dH_{eff}}\right)\right)\left(\frac{dM}{dH}\right)-\left(M_{an}-M+k\delta c\frac{dM_{an}}{dH_{eff}}\right)=0. \tag{2}$$

In this equation, μ_0 is the permeability of free space, d is a dimension of the material (diameter for cylinders, thickness for laminations), ρ is the resistivity of the material, β is a geometry factor (6 for laminations, 16 for cylinders), G is a dimensionless constant, w is the width of laminations, H_0 is a parameter related to domain walls, k is related to the hysteresis, δ is +1 or −1 depending on the sign of dH, c is the reversibility coefficient, and M_{an} is the local anhysteretic magnetization. A Langevin function is used to model the local anhysteretic magnetization,

$$M_{an}(t,x)=M_s\left[\coth\left(\frac{H_{eff}(t,x)}{a}\right)-\frac{a}{H_{eff}(t,x)}\right], \tag{3}$$

where M_s is the saturation magnetization, a controls the slope of the anhysteretic magnetization, and H_{eff} is the effective magnetic field. The effective magnetic field includes the applied magnetic field H, the Weiss mean field interactions αM, and magnetoelastic interactions $H\sigma$ as follows,

$$H_{eff}(t,x)=H(t,x)+\alpha M(t,x)+H_\sigma(t,x). \tag{4}$$

Magnetoelastic interactions depend on the stress state of the material and the magnetostriction λ as follows,[18]

$$H_\sigma(t,x)=\frac{3}{2\mu_0}\left[\sigma\frac{\partial\lambda}{\partial M}+\lambda\frac{\partial\sigma}{\partial M}\right]. \tag{5}$$

2.2 Magnetomechanical effect

The contribution of stress to the total magnetization, $dM/d\sigma$, must now be considered. A theory describing the magnetomechanical effect based on freeing of domain walls has been presented previously.[19] The "law of approach" is based on the idea that changes in stress force the total magnetization to approach the anhysteretic magnetization,

$$\frac{\partial M}{\partial\sigma}=\frac{\sigma}{E\xi}\left(\overline{M}_{an}-M\right)+c\frac{\partial\overline{M}_{an}}{\partial\sigma}, \tag{6}$$

where E is Young's modulus of Terfenol-D, ξ is a coefficient to be identified experimentally, and $\overline{M}_{an}$ is the global anhysteretic magnetization. The global anhysteretic magnetization is found by solving iteratively Equation 3,

$$\overline{M}_{an}=M_s\left[\coth\left(\frac{H+\overline{\alpha}\left(\overline{M}_{an},\sigma\right)\overline{M}_{an}}{a}\right)-\left(\frac{a}{H+\overline{\alpha}\left(\overline{M}_{an},\sigma\right)\overline{M}_{an}}\right)\right]. \tag{7}$$

It is noted that the effective filed is here expressed $H_{eff}=H+\overline{\alpha}(M,\sigma)M$, where $\overline{\alpha}$ is a mean interaction coefficient of the form

$$\bar{\alpha} = \alpha + \frac{3}{2\mu_0}\left[\sigma\frac{\partial\lambda}{\partial M} + \lambda\frac{\partial\sigma}{\partial M}\right]. \tag{8}$$

2.3 Magnetostriction model

For the general case, a relationship between magnetostriction and magnetization cannot be determined. However, in the case where the magnetic moments are forced to align perpendicular to the direction of applied field, a relationship can be identified. For polycrystalline materials such as Terfenol-D, this alignment can be accomplished by proper crystal growth during manufacturing and by applying a sufficiently large preloading during operation. In this case the dominant magnetization process is domain wall rotation and energy minimization results in the single-valued quadratic law $\lambda=3\lambda_s M^2/2M_s^2$.

An alternative, but not unrelated, approach consists of formulating an empirical model based on a series expansion symmetric about M = 0,

$$\lambda(M) = \sum_{i=0}^{\infty}\gamma_i M^{2i}, \tag{9}$$

where the coefficients γ_i are determined from experimental data.[19] The series is often truncated after i=1, yielding a model equivalent to the quadratic law. Here the model will be truncated after i=2, yielding a quartic law. The coefficients γ_1 and γ_2 of the quartic model are identified by solving the constraints at magnetic saturation and at the inflection point M_0,

$$\begin{aligned}\lambda(M_s) &= \gamma_1 M_s^2 + \gamma_2 M_s^4 = \lambda_s \\ \frac{\partial^2\lambda}{\partial M^2} &= 2\gamma_1 + 12\gamma_2 M_0^2 = 0.\end{aligned} \tag{10}$$

More sophisticated models capable of including hysteresis effects are available.[20] However, the quartic model provides sufficient accuracy for the work described here.

2.4 Transducer structural dynamics

The magnetostriction given by Equation 10 quantifies the reorientation of magnetic moments towards the direction of the applied field. However, it ignores the elastic properties of the magnetostrictive material as it vibrates. In this section a partial differential equation (PDE) system is formulated which models the elastic response of the magnetostrictive material and other transducer components. The input to this PDE is formulated through the magnetostriction λ which constitutes an internal force causing vibrations of the transducer. The solution to the PDE is the longitudinal displacement as a function of time and position relative to the prestressed position. Additional details regarding this formulation are described by Dapino.[14]

Figure 1 shows a schematic of the transducer with the major mechanical and electromagnetic components. The structural dynamics are modeled through consideration of the Terfenol-D rod, the flexure top, the preload spring, and the output push rod. Both the flexure top and preload spring provide a compressive load to the Terfenol-D. These components are represented by a linear spring k_p and a dashpot c_p in Figure 2. The Terfenol-D rod has a length L, cross sectional area A, material density ρ, elastic modulus E, internal damping c_D, and longitudinal coordinate x. The external mass load is represented by the point mass m_p.

The total stress in the rod is given by the expression,

$$\sigma = E\frac{\partial u}{\partial x} + c_D\frac{\partial^2 u}{\partial x\partial t} - E\lambda + \sigma_0, \tag{11}$$

where the terms on the right hand side represent linear elasticity at small displacements, Kelvin-Voigt damping, magnetostriction-derived stress, and prestress. Force balancing then yields the dynamic model for longitudinal displacements and strains.

For implementation, the model is formulated in a weak or variational form by multiplying the strong form by test functions ϕ, and integrating through the length of the rod. Details on the requirements of the test functions and the solution of the model can be found in Dapino.[14] The weak form of the dynamic model is

$$\int_0^L \rho A \frac{\partial^2 u}{\partial t^2}\phi dx = -\int_0^L \left[EA\frac{\partial u}{\partial x} + C_D A \frac{\partial^2 u}{\partial x \partial t} - EA\lambda \right] \frac{\partial \phi}{\partial x} dx$$
$$- \left[k_p u(t,L) + c_p \frac{\partial u}{\partial t}(t,L) + m_p \frac{\partial^2 u}{\partial t^2}(t,L) \right] \phi(L). \tag{12}$$

The solution to Equation 12 defines the longitudinal displacements about the prestressed position. Strains are evaluated by taking derivatives with respect to position and the material stresses are then computed from Equation 11.

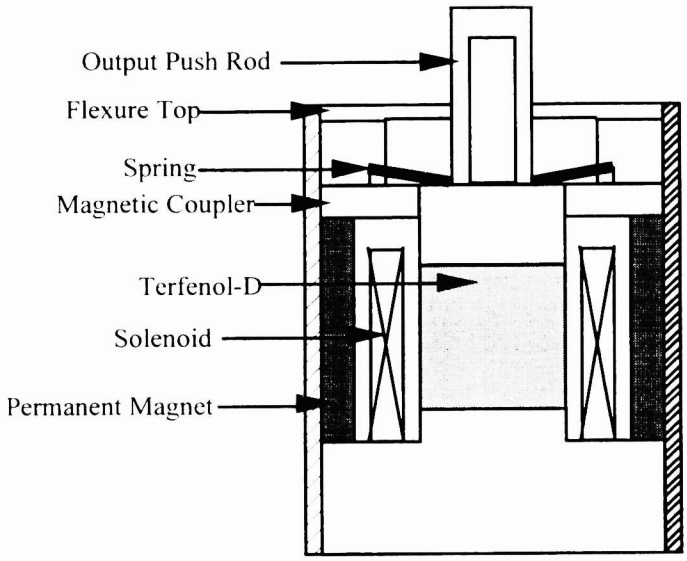

Figure 1. Schematic of ETREMA AU-008 ultrasonic transducer.

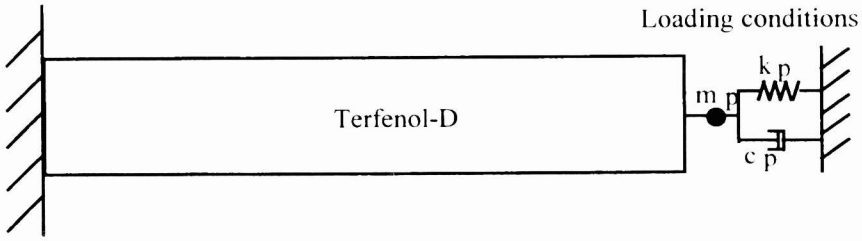

Figure 2. Structural dynamics model of the ultrasonic transducer.

2.5 Model summary

Table 1 shows a summary of the equations used in the transducer model. An iterative approach to solving the equations must be followed, as the stress state and magnetization of the material cannot be determined independently. Many of the parameters used in the equations are readily identified from published sources or geometry. Others must be identified experimentally. The parameters to be identified include: M_s, M_0, λ_s, a, k, α, c, and ξ.

Equation	Description
$\frac{dM}{dt} = \frac{\partial M}{\partial H}\frac{dH}{dt} + \frac{\partial M}{\partial \sigma}\frac{d\sigma}{dt}$	Rate of change of magnetization with time.
$\left(\frac{\mu_0 d^2}{2\rho\beta}\frac{dH}{dt}\right)\left(\frac{dM}{dH}\right)^2 + \left(\frac{GdwH_a}{\rho}\right)^{1/2}\left(\frac{dH}{dt}\right)^{1/2}\left(\frac{dM}{dH}\right)^{3/2} + \left(k\delta - \alpha\left(M_{an} - M + k\delta c\frac{dM_{an}}{dH_{eff}}\right)\right)\left(\frac{dM}{dH}\right) - \left(M_{an} - M + k\delta c\frac{dM_{an}}{dH_{eff}}\right) = 0$	Frequency dependent differential susceptibility.
$M_{an}(t,x) = M_s\left[\coth\left(\frac{H_{eff}(t,x)}{a}\right) - \frac{a}{H_{eff}(t,x)}\right]$	Anhysteretic magnetization.
$H_{eff}(t,x) = H(t,x) + \alpha M(t,x) + H_\sigma(t,x)$	Effective magnetic field.
$H_\sigma(t,x) = \frac{3}{2\mu_0}\left[\sigma\frac{\partial\lambda}{\partial M} + \lambda\frac{\partial\sigma}{\partial M}\right]$	Magnetoelastic magnetic field.
$\frac{\partial M}{\partial \sigma} = \frac{\sigma}{E\xi}\left(\overline{M}_{an} - M\right) + c\frac{\partial \overline{M}_{an}}{\partial \sigma}$	Law of approach.
$\overline{M}_{an} = M_s\left[\coth\left(\frac{H + \overline{\alpha}\left(\overline{M}_{an},\sigma\right)\overline{M}_{an}}{a}\right) - \left(\frac{a}{H + \overline{\alpha}\left(\overline{M}_{an},\sigma\right)\overline{M}_{an}}\right)\right]$	Global anhysteretic magnetization.
$\overline{\alpha} = \alpha + \frac{3}{2\mu_0}\left[\sigma\frac{\partial\lambda}{\partial M} + \lambda\frac{\partial\sigma}{\partial M}\right]$	Interaction coefficient.
$\lambda(M) = \sum_{i=0}^{\infty}\gamma_i M^{2i}$	Magnetostriction.
$\lambda(M_s) = \gamma_1 M_s^2 + \gamma_2 M_s^4 = \lambda_s$ $\frac{\partial^2\lambda}{\partial M^2} = 2\gamma_1 + 12\gamma_2 M_0^2 = 0$	Constraints on quartic magnetostriction model.
$\sigma(t) = E\frac{\partial u}{\partial x} + c_D\frac{\partial^2 u}{\partial x \partial t} - E\lambda + \sigma_0$	Stresses in the Terfenol-D.
$\int_0^L \rho A\frac{\partial^2 u}{\partial t^2}\phi\,dx = -\int_0^L\left[EA\frac{\partial u}{\partial x} + C_D A\frac{\partial^2 u}{\partial x\partial t} - EA\lambda\right]\frac{\partial\phi}{\partial x}dx - \left[k_p u(t,L) + c_p\frac{\partial u}{\partial t}(t,L) + m_p\frac{\partial^2 u}{\partial t^2}(t,L)\right]\phi(L)$	Dynamic transducer model.

Table 1. Summary of transducer model equations.

3. EXPERIMENTAL VERIFICATION

In this section, model simulations and experimental results are compared for a standard ETREMA AU-008 ultrasonic transducer, whose configuration follows that of Figure 1. The transducer consists of a 0.5" diameter by 0.5" long laminated Terfenol-D rod with a reaction mass on one end and a push rod on the other. The transducer includes a permanent magnet to

provide a magnetic bias field. The permanent magnet was demagnetized as appropriate to achieve unbiased operation. A compressive stress of 1500 psi is applied to the Terfenol-D via a Belleville spring and housing. The output push rod is threaded for easy attachment to various loads.

For model verification purposes, a fixed-free configuration was simulated experimentally by attaching the transducer to a massive table. The attachment bolt between the transducer and table was nonmagnetic and significantly stiffer than any of the transducer components.

The tests were run at fixed-frequency sinusoidal input current to the actuator. Data collected included current, voltage, flux density, and displacement. A linear amplifier operating in current-controlled mode was used to drive the actuator. A 25-turn pickup coil wound around the Terfenol-D rod was used to compute the magnetic induction, B. The voltage signal from this coil was fed into an integrating voltmeter calibrated so that $B = -(1/A)\int V dt$, with A the cross sectional area of the rod. The output rod displacement was measured with a photonic sensor. Magnetic field and flux density were used to calculate the magnetization of the Terfenol-D, $B=\mu_0(H+M)$. Applied magnetic field, H, was computed from the input current using a coil rating (magnetic field per unit current) established by measuring the magnetic field in the coil with a Hall probe for various input currents. Finite element simulations of the magnetic circuit using a nonlinear B-H curve for the Terfenol-D showed that the magnetic field in the material deviates from a true sinusoid at low field levels near where the current crosses zero. This discrepancy may account for some slight deviations between model and experiment at low magnetic fields.

3.1 Magnetically unbiased tests

Magnetically unbiased testing allows the model to be validated over both positive and negative values of H. Input to the transducer was a sinusoidal current at a specified frequency. The magnetic field was assumed to be proportional to the current. Tests were run at various frequencies from 1 Hz to 30 kHz. The low frequency tests were run at magnetic field amplitudes nearly up to saturation, however, because of amplifier limitations, the high frequency tests were run at lower amplitudes.

Experimental and model curves for magnetization and strain are shown in Figure 3 and Figure 4 for operation at 1 Hz and input level of 110 kA/m. The parameters in the model were optimized to achieve accurate characterization of both the magnetization and strain. A very accurate characterization of the experimental results was achieved for both the magnetization and the strain. For the magnetization there are slight deviations at low magnetic field levels due to the method of measuring H and slight deviations at high magnetic fields. The strains show a slight difference in slope and deviations at high magnetic fields. For a magnetically unbiased actuator operating at 1 Hz, the model provides an excellent representation of the experimental results.

Magnetization and strain curves for the unbiased transducer operating at 1 kHz with a 20 kA/m sinusoidal magnetic excitation are shown in Figures 5 and 6. Model parameters were optimized for best fit of the experimental results. The model provides excellent characterization of the experimental magnetization and strain. There are some discrepancies at very low magnetic fields and at higher magnetic fields. Some of the low field discrepancies arise from the method of calculating magnetic field. The discrepancies in the strain may be due to uncharacterized dynamic components in the transducer such as spring rates and damping.

3.2 Magnetically biased tests

Verification tests were run with the permanent magnets in the transducer magnetized, so the transducer was in a magnetically biased state. Magnetically biased operation is the typical use of this ultrasonic transducer. Input to the transducer was a sinusoidal current at a specified frequency. Magnetic field was assumed to be proportional to the current. Tests were run at various frequencies from 1 Hz to 30 kHz. Amplitude of the input current was limited by the magnetic bias field for low frequencies. The amplitude of the applied magnetic field never exceeded the magnetic bias field. At high frequencies, the input current was limited by the amplifier capabilities.

Experimental and model magnetization for 1 Hz operation is shown in Figure 7. Model parameters were optimized to achieve an accurate characterization of the magnetization. While the slope of the magnetization is accurately characterized by the model, the amount of magnetic hysteresis is overpredicted by the model. Deviation between experiment and model may be due to inaccurate characterization of the magnetic bias field. In spite of some deviations, the model provides a reasonable characterization of the experimental magnetization.

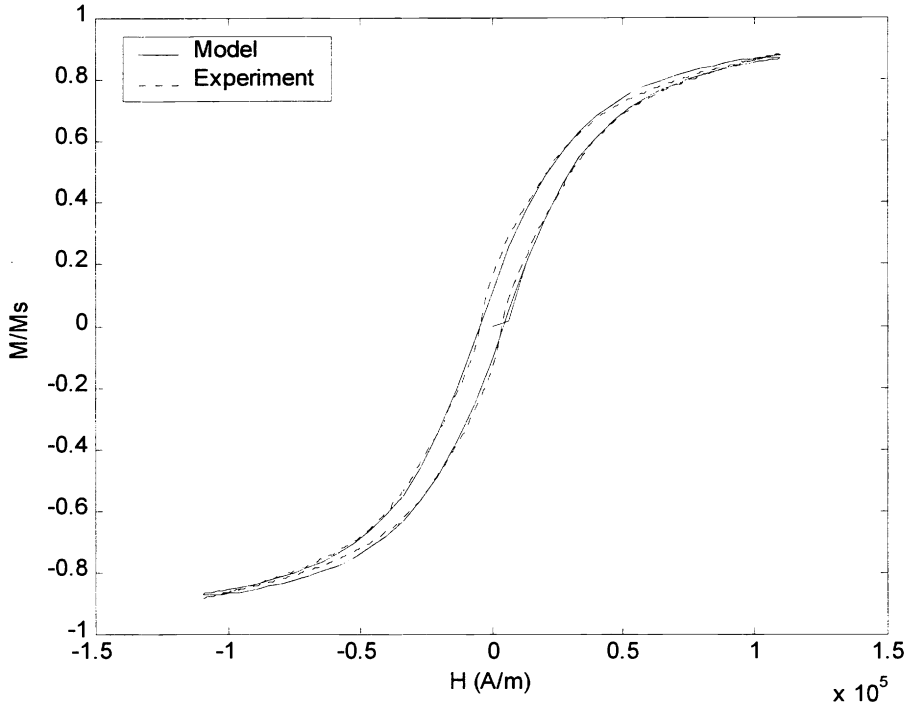

Figure 3. Relative magnetization M/M_s versus applied field H, 1Hz frequency excitation, 25 A input current (110 kA/m magnetic field), unbiased.

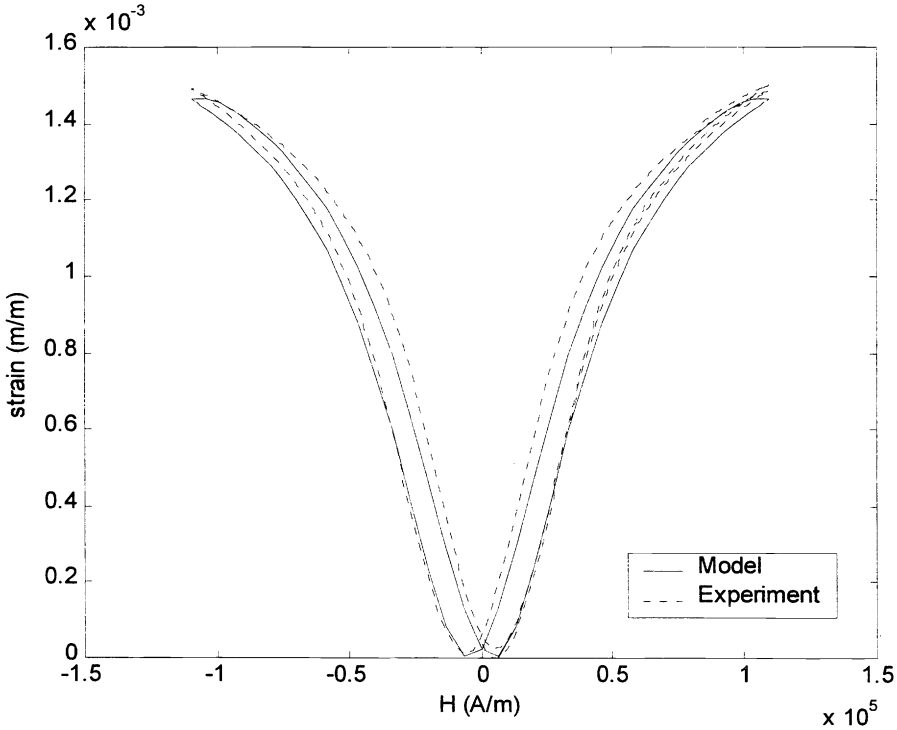

Figure 4. Strain versus applied field H, 1Hz frequency excitation, 25 A input current (110 kA/m magnetic field), unbiased.

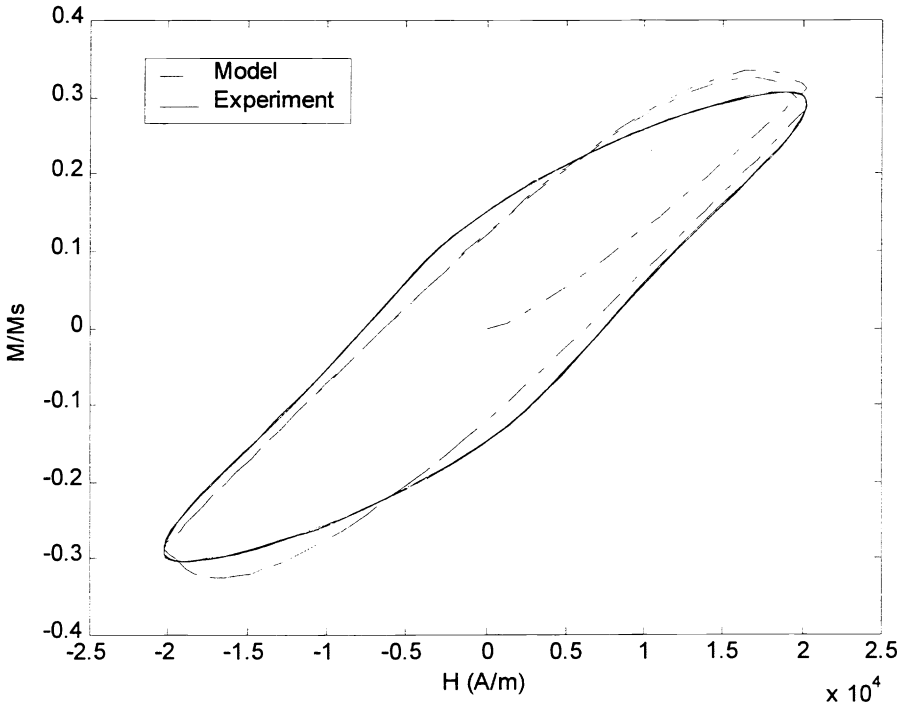

Figure 5. Relative magnetization M/M_s versus applied field H, 1kHz frequency excitation, 5 A input current (20 kA/m magnetic field), unbiased.

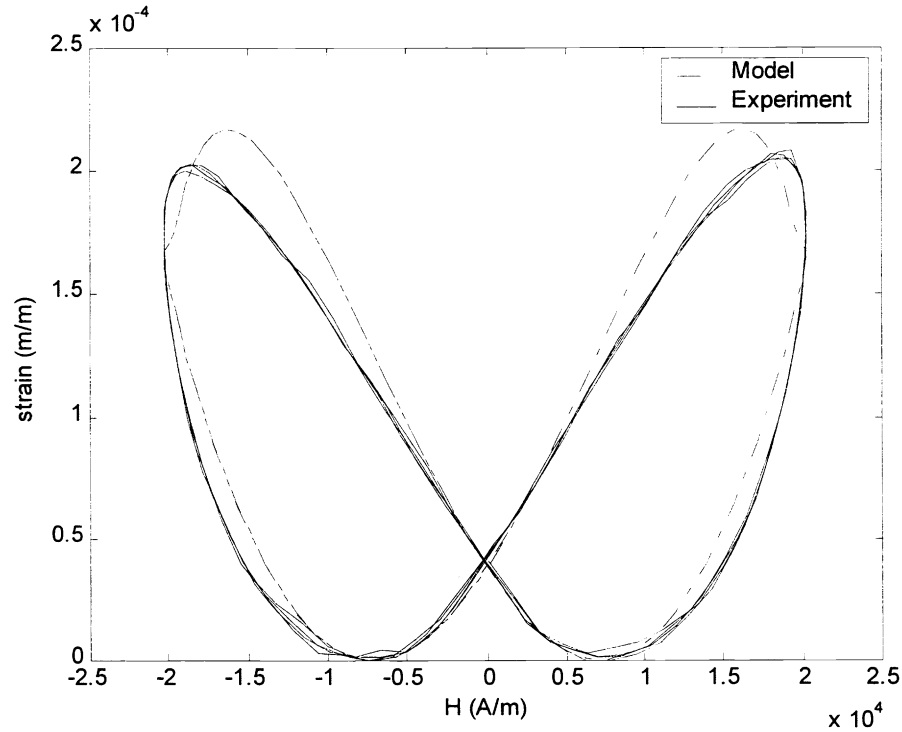

Figure 6. Strain versus applied field H, 1kHz frequency excitation, 5 A input current (20 kA/m magnetic field), unbiased.

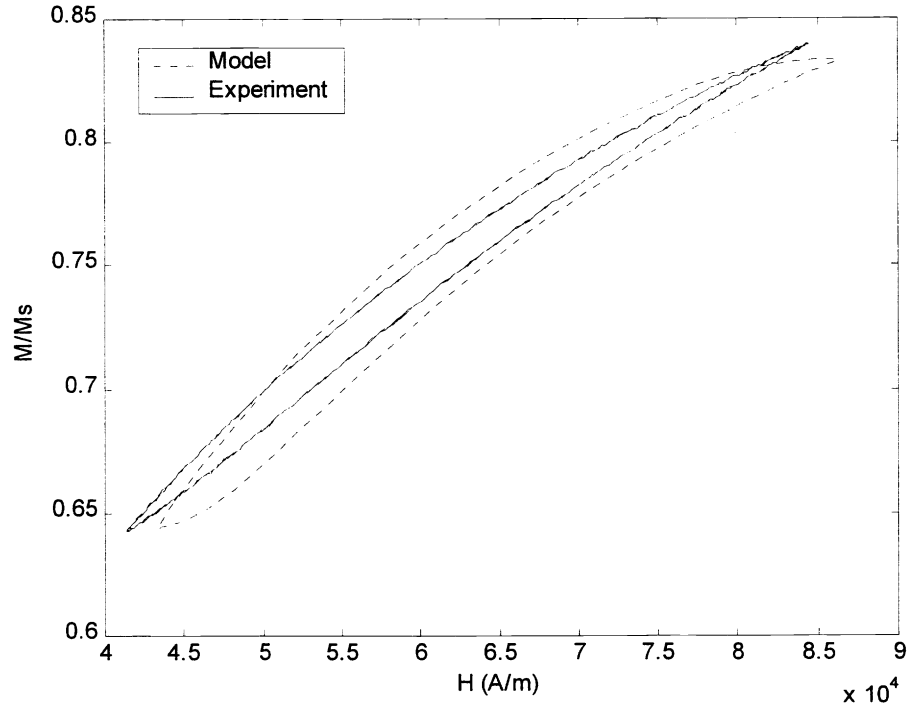

Figure 7. Relative magnetization M/M_s versus applied field H, 1 Hz frequency excitation, 5 A input current (25 kA/m magnetic field), biased actuator.

For 23 kHz operation, the slope and width of the magnetization were very accurately represented by the model, Figure 8. Model parameters were optimized to achieve accurate characterization of the magnetization. There is some deviation after the magnetic field has reversed direction. The model provides very accurate representation of the experimental magnetization for operation of a magnetically biased transducer at 23 kHz.

3.3 Summary of experimental verification

Table 2 shows the optimized parameters used in the model for each of the drive conditions. For the unbiased actuator the same parameters were used at both 1 Hz and 1 kHz. Similarly, for the biased actuator the same parameters were used for both 1 Hz and 23 kHz. However, there are some mechanical parameters that were changed slightly in the biased cases such as Young's modulus and damping factors. More work needs to be done to determine a single set of parameters that would accurately characterize both magnetization and strain for all operating conditions.

Freq. (Hz)	Biased (Y/N?)	M_s (10^4)	M_0 (10^3)	λ_s (10^{-6})	a (10^4)	k	c	α	ξ (10^3)
1	N	7.65	1.2	1950	1.25	6000	0.10	0.082	5
1000	N	7.65	1.2	1950	1.25	6000	0.10	0.082	5
1	Y	7.65	1.0	1800	1.0	6000	0.23	0.075	5
23000	Y	7.65	1.0	1800	1.0	6000	0.23	0.075	5

Table 2. Parameters used for various operating conditions.

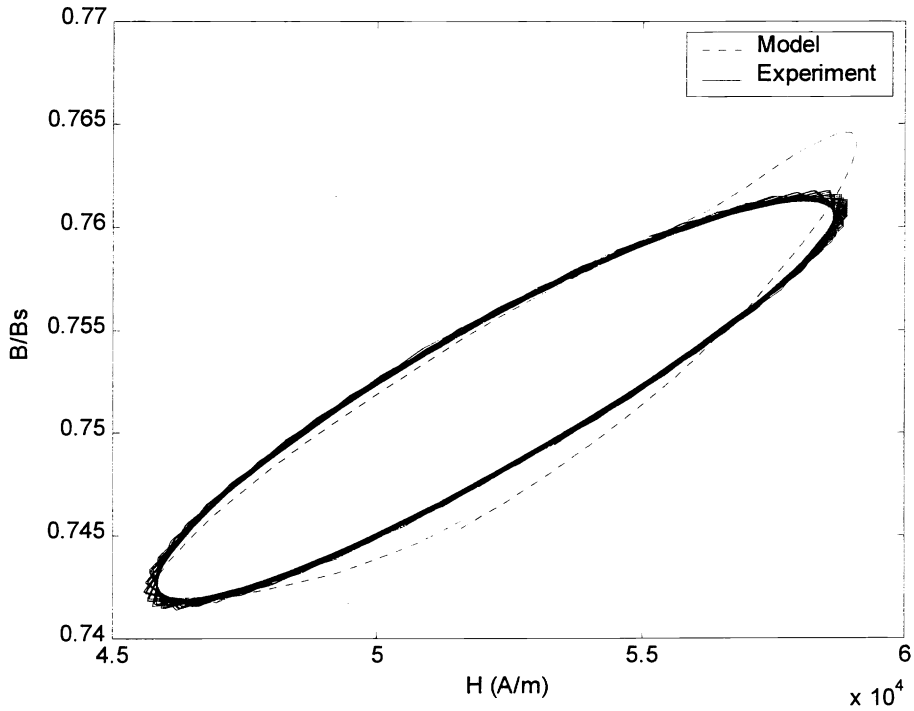

Figure 8. Relative magnetization M/M_s versus applied field H, 23 kHz frequency excitation, 5 A input current (10 kA/m magnetic field), biased actuator.

4. CONCLUSIONS

A magnetoelastic model for magnetostrictive transducers was employed to characterize the behavior of a Terfenol-D ultrasonic transducer. Validation of the model was performed using an actuator in unbiased and biased conditions over a wide variety of operating conditions. In its present configuration, the model provides a good characterization of the behavior of Terfenol-D transducers operating in an unbiased or biased state with low or high drive levels at any frequency.

Discrepancies between the model and experiments may be due to lack of characterization of the dynamic components of the transducer such as spring loads and damping factors. Another cause for discrepancies may the approximate nature of the strain model. A third possible cause of discrepancies is the error in the measured applied magnetic field near zero. At this time, one set of model parameters cannot accurately represent the transducer operation over the entire frequency range of DC to 30 kHz. However, over smaller frequency ranges, constant sets of parameters accurately model the transducer behavior.

In its present state, the model characterizes the experimental magnetization quite accurately, but is less than optimal for predicting strain output of the biased transducer. Characterization over a broader range of operating conditions such as different nominal preload and large external loads will result in improved parameter identification. Additional improvements may also be achieved through improved minor loop closure techniques.

ACKNOWLEDGEMENTS

The authors would like to thank the NIST Advanced Technology Program and the National Science Foundation for their support of this work. The work of R.C.S. was supported in part by the Air Force Office of Scientific Research.

REFERENCES

1. J. R. Frederick, *Ultrasonic Engineering*, John Wiley & Sons, Inc., New York, 1965, pp. 60-85.
2. A. E. Crawford, *Ultrasonic Engineering with Particular Reference to High Power Applications*, Academic Press Inc., New York, 1955, pp. 47-112.
3. M. J. Dapino, F. T. Calkins, and A. B. Flatau, "Magnetostrictive Devices," *Wiley Encyclopedia of Electrical and Electronics Engineering*, New York, 1999, pp. 292-294.
4. NIST Advanced Technology Program, *Terfenol-D High Power Ultrasonic Transducer*, NIST Grant No. 97-01-0023.
5. T. A. Duenas, L. Hsu, and G. P. Carman, "Magnetostrictive composite material systems analytical/experimental," *Advanced Smart Materials Fundamentals and Applications*, Boston, MA, 1996.
6. G. P. Carman and M. Mitrovic, " Nonlinear constitutive relations for magnetostrictive materials with applications to 1-D problems," *Journal of Intelligent Materials Systems and Structures*, **6**, pp. 673-684, 1995.
7. K. S. Kannan and A. Dasgupta, "Continuum magnetoelastic properties of Terfenol-D; what is available and what is needed," in *Adaptive Materials Symposium, Summer Meeting of ASME-AMD-MD*, UCLA, 1995.
8. J. B. Restorff, H. T. Savage, A. E. Clark, and M. Wun-Fogle, "Preisach modeling of hysteresis in Terfenol-D," *J. Appl. Phys.*, **67**(9), pp. 5016-8, 1990.
9. A. A. Adly and I. D. Mayergoyz, "Magnetostriction simulation using anisotropic vector Preisach-type models," *IEEE Trans. Magn.* **32**(5), pp. 4473-5, 1996.
10. R. C. Smith, "Modeling techniques for magnetostrictive actuators," *Proceedings of SPIE Symposium on Smart Structures and Materials*, Vol. 3041, pp. 243-253, San Diego, CA, 1997.
11. G. Engdahl and A. Berqvist, "Loss simulations in magnetostrictive actuators," *J. Appl. Phys.* **79**(8), pp. 4689-91, 1997.
12. V. Basso and G. Bertotti, "Hysteresis models for the description of domain wall motion," *IEEE Trans. Magn.* **32**(5), pp. 4210-12, 1996.
13. F. T. Calkins, *Design, analysis, and modeling of giant magnetostrictive transducers*, Iowa State University, Ph.D. Thesis, Ames, IA, 1999.
14. M. J. Dapino, *Nonlinear and hysteretic magnetomechanical model for magnetostrictive transducers*, Iowa State University, Ph.D. Thesis, Ames, IA, 1999.
15. M. J. Dapino, F. T. Calkins, R. C. Smith, and A. B. Flatau, "A magnetoelastic model for magnetostrictive sensors," *Proceedings of ACTIVE 99*, Fort Lauderdale, FL, 1999 (to appear).
16. D.C. Jiles and D. L. Atherton, "Theory of ferromagnetic hysteresis," *J. Magn. Magn. Mater.*, **61**, pp. 48-60, 1986.
17. D. C. Jiles, "Modelling the Effects of Eddy Current Losses on Frequency Dependent Hysteresis in Electrically Conducting Media," *IEEE Trans. Magn.*, **30**(6), pp.4326-28, 1994.
18. M. J. Sablik and D. C. Jiles, "Coupled magnetoelastic theory of magnetic and magnetostrictive hysteresis," *IEEE Trans. Magn.*, **29**(3), pp. 2113-23, 1993.
19. D. C. Jiles, "Theory of the magnetomechanical effect," *J. Phys. D: Appl. Phys.* **28**, pp. 1537-1546, 1995.
20. M. J. Sablik and D. C. Jiles, "A model for hysteresis in magnetostriction," *J. Appl. Phys.*, **64**(10), pp. 5402-04, 1988.